coatings

MDPI

Communication

Effect of Electric Properties according to Volume Ratio of Supercapacitor and Battery Capacitor in Hybrid Energy Storage System

Jong-Kyu Lee and Jung-Rag Yoon *

R&D Center, SAMWHA CAPACITOR, Yongin 17118, Republic of Korea; jklee@samwha.com
* Correspondence: yoonjungrag@samwha.com

Abstract: The development of technology that combines supercapacitors and lithium-ion batteries by externally connecting them in parallel is ongoing. This study examines the correlation between the volume ratio and electrical characteristics of a cell made by internally connecting a battery capacitor with $Li_4Ti_5O_{12}$ as the anode active material and a supercapacitor in parallel. It was found that increasing the volume occupied by the battery capacitor in the cell led to increased cell energy and resistance, resulting in decreased output characteristics. Conversely, increasing the volume occupied by the supercapacitor in the cell led to a decrease in the IR drop during discharge and the cell temperature when evaluating cycle characteristics with a current of 20C. This study also examined the behavior of the current distributed during the charging and discharging process based on the volume ratio of the supercapacitor and the battery capacitor. Analyzing the correlation between the volume ratio and electrical characteristics of supercapacitors and battery capacitors could potentially lead to the development of a new type of energy storage device.

Keywords: battery capacitor; supercapacitor; hybrid energy storage system; L-ion battery; $Li_4Ti_5O_{12}$

check for updates

Citation: Lee, J.-K.; Yoon, J.-R. Effect of Electric Properties according to Volume Ratio of Supercapacitor and Battery Capacitor in Hybrid Energy Storage System. *Coatings* **2023**, *13*, 1316. https://doi.org/10.3390/coatings13081316

Academic Editor: Wei Xu

Received: 10 June 2023
Revised: 25 July 2023
Accepted: 25 July 2023
Published: 27 July 2023

1. Introduction

Supercapacitors and lithium-ion batteries are widely used energy storage devices. Lithium-ion batteries achieve capacity by intercalating and the deintercalation Li-ions into and out of the crystal structure of the cathode and anode materials. On the other hand, supercapacitors achieve capacitance by adsorbing and desorbing ions from the electrolyte solution on the surface of activated carbon, which is an electrode material. These two energy storage devices have significant differences in their properties due to their different reaction mechanisms. Supercapacitors have a low energy density, but their lifespan and output characteristics are significantly higher than those of lithium-ion batteries. Conversely, batteries have a much higher energy density compared to supercapacitors [1–10].

Supercapacitors possess a voltage range of 0 to 2.7 volts, while lithium-ion batteries typically exhibit a voltage range of 3.0 to 4.2 volts. Active materials such as activated carbon, carbon nanotubes, and graphene are utilized in supercapacitors. Upon the application of voltage, the ions of the electrolyte undergo continuous adsorption and desorption on the surface of the active material. [11,12] The operational voltage of a supercapacitor ranges from 0 to 2.7 V. However, internally, voltages of 4.2 to 4.3 V for the anode and 1.5 to 1.6 V for the cathode are employed. Consequently, when an operational voltage of 4.2 V is applied, similar to that of a lithium-ion battery, the cathode experiences an internal voltage rise of nearly 5 V, resulting in the decomposition of the electrolyte and a potential cell explosion caused by gas. Conversely, in a lithium-ion battery, the anode reacts with lithium near 4.2 V, while the cathode does so near 0 V, leading to a typical operating voltage of 4.2 V. Additionally, supercapacitors have a high-power density and can deliver high bursts of power. They also have a relatively short discharge time, typically on the order of a few seconds. Lithium-ion batteries, on the other hand, have a high energy density and can deliver power over a longer period of time, typically from hours to days [13,14].

By combining supercapacitors and lithium-ion batteries, the resulting hybrid energy storage system can take advantage of the strengths of both technologies. Supercapacitors can provide high power density and fast discharge times, while lithium-ion batteries can provide high energy density and longer discharge times. The voltage ranges of these two components can also be matched to allow for a smooth and efficient transfer of energy between the supercapacitors and lithium-ion batteries as needed.

Research is currently underway to enhance the longevity of lithium-ion batteries through the production of lithium-ion battery modules and parallel connection of supercapacitor modules, aiming to alleviate the load placed on the batteries. This strategy arises from the fact that the reaction voltages of individual cells within the supercapacitor and lithium-ion battery differ, rendering a 1:1 series connection impractical. Thus, a modularized approach is adopted, wherein voltage matching is implemented.

Conventionally, the anode material of a lithium-ion battery consists of graphite. However, it is noteworthy that a battery capacitor utilizing $Li_4Ti_5O_{12}$ (LTO) as an anode in lieu of graphite can also be classified as a type of lithium-ion battery [15,16]. LTO exhibits a potential of approximately 1.55 V, resulting in an operating voltage range of 1.5 V to 2.7 V. Given that these battery capacitors share the same maximum operating voltage as supercapacitors, they can be effectively integrated by connecting cells in a series.

Most studies on combining supercapacitors and lithium-ion batteries are conducted at the module level; however, battery capacitors have a similar voltage range to supercapacitors, allowing them to be connected in parallel between cells. This makes the battery capacitor a candidate for transforming into a new type of energy storage device. By combining supercapacitors and battery capacitors, the system's efficiency can be improved, and the lifetime characteristics can be improved by reducing the burden on the battery capacitor at a high current. This results in a new energy storage device that is capable of both long-term energy storage and high-power transmissions. Additionally, the combination of supercapacitors and battery capacitors can provide high-performance energy storage while reducing the overall cost of an energy storage system [17–28].

It is important to note that the specific voltage range and discharge time for a hybrid energy storage system depends on the specific components used, as well as the configuration of the system. However, in general, hybrid energy storage systems that combine supercapacitors and battery capacitors can offer improved performance and efficiency compared to using either technology alone.

In this study, we aimed to investigate the improvement of system efficiency, reliability, performance, and cost-effectiveness by combining supercapacitors and battery capacitors in the same cell with a specific volume ratio.

2. Materials and Methods

2.1. Fabrication of Individual Cells

For the positive electrode of the battery capacitor, an electrode slurry was prepared by mixing two types of $Li(Ni_{1/3}Co_{1/3}Mn_{1/3})O_2$ (NCM) and $LiCoO_2$ (LCO) positive electrode active materials, with super-p serving as a conductive material and Poly(vinylidene fluoride) (PVdF) as a binder, in a mixing ratio of 87:6.5:6.5 with NMP used as a solvent. For the anode of the battery capacitor, a slurry was prepared using $Li_4Ti_5O_{12}$ (LTO) as the active material with the same ratio of the binder and conductive material as the cathode. The positive and negative electrodes were coated on etched Al foil with a thickness of 20 μm and were subjected to a roll press to manufacture the positive and negative electrodes, with approximately 25% compression. The resulting electrodes were then formed into a jelly roll using a winding machine, dried at 145 °C for 48 h, and impregnated with a 1.0M $LiPF_6$ + (ethylene carbonate) EC/dimethyl carbonate (DMC)/ethyl methyl carbonate (EMC) (1:1:1) electrolyte solution to assemble the cell.

The supercapacitor utilized activated carbon as the electrode active material, super-P as the conductive material, and a binder consisting of a mixture of carboxymethyl cellulose (CMC), styrene-butadiene rubber (SBR), and poly(tetrafluoroethylene) (PTFE). The electrode slurry was prepared with a ratio of 80:10:10 for the active material, conductive material, and binder, respectively. The electrodes were coated on etched Al foil with a thickness of 20 µm and were produced by a roll press with approximately 15% compression. The fabricated electrodes were then formed into a jelly roll using a winding machine, dried at 145 °C for 48 h, and impregnated with a 1.0M $TEABF_4$ + acetonitrile (ACN) electrolyte solution to assemble a cell.

2.2. Complex Cell Fabrication

The electrolyte of the battery capacitor used $LiPF_6$ salt, the supercapacitor used $TEABF_4$ salt, and other types of solvents were also utilized. To connect the battery capacitor and the supercapacitor in parallel within a single cell, it was necessary to insert a separation layer to prevent the mixing of electrolytes. Urethane was selected as the separation layer material, as it was determined to be suitable due to the absence of any reaction when immersed in both the battery capacitor electrolyte and the supercapacitor electrolyte. The presence of a separation layer ensured that no reaction took place at the interface between the battery capacitor and the supercapacitor during the charging and discharging of the composite cell. This allowed for independent charging and discharging processes to take place.

Table 1 shows the volume and capacity ratios of the supercapacitor and battery capacitor. Figure 1 presents a schematic diagram of the combination of a battery capacitor and a supercapacitor, showing the volume ratio and capacity ratio. The battery capacitor had a capacity that was approximately 17 times higher than that of the supercapacitors at the same volume, resulting in differences in capacity among the cells depending on the volume ratio. Single battery capacitors and supercapacitors that have not been combined were also compared to composite cells.

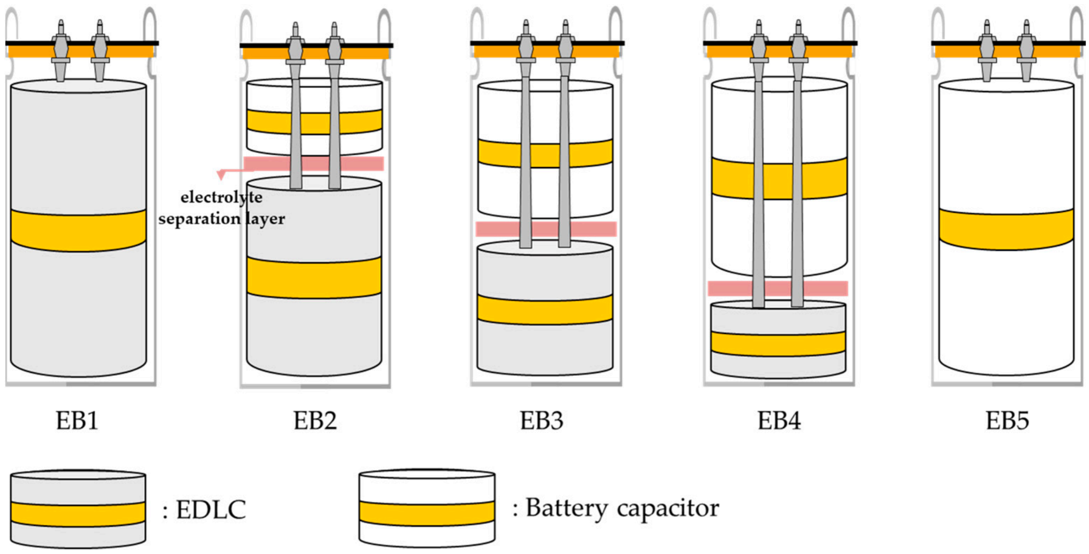

Figure 1. Schematic diagram of complex cell structure according to individual cell and volume ratio of battery capacitor and supercapacitor.

Table 1. The properties of the complex cell structure according to individual cell and volume ratio of battery capacitor and supercapacitor.

	EB1	EB2	EB3	EB4	EB5
Supercapacitor (F)	872.3	654.3	436.2	218.0	-
Battery capacitor (F)	-	3801.6	7603.2	11,404.8	16,203.0
Volume ratio occupied by EDLC (%)	100	75	50	25	0
Capacity ratio occupied by EDLC (%)	100	14.7	5.4	1.9	0

2.3. Cell Evaluation

The capacity and resistance characteristics of battery capacitors, supercapacitors, and composite cells were assessed by applying charge and discharge currents ranging from 1 A to 20 A within the voltage range of 1.5 V to 2.7 V at room temperature. An Arbin charger and discharger were employed for this evaluation. Additionally, a long-term life evaluation was conducted by subjecting each cell to a current of 20C at room temperature. The surface temperature of the cell was measured using a thermal imaging camera during the 20C current evaluation to assess the cell lifetime. Furthermore, an oscilloscope was utilized to evaluate the current distribution flowing through the battery capacitor and supercapacitor during the charging and discharging processes of the composite cell.

3. Results

Figure 2 shows the capacitance and resistance of the individual battery capacitor and supercapacitor cells, as well as the composite cell, which was measured by applying a current of 1 A at 2.7~1.5 V. The composite cell's capacity decreased as the volume ratio of the battery capacitor increased because the battery capacitor's capacity was about 17 times larger than that of the supercapacitor. When cells are manufactured with the same volume, the resistance of a battery capacitor is approximately 3.3 times greater than that of a supercapacitor. Consequently, as the volume fraction of the battery capacitor within the total cell increases, the resistance also increases. The lower resistance observed in EB5, which is a cell consisting solely of a battery capacitor, compared to EB4, a composite cell comprising both a supercapacitor and a battery capacitor, cpi;d be attributed to the increased contact resistance resulting from the internal connection between the supercapacitor and battery capacitor in the EB4 cell. Please refer to Figure 1 for the visualization of the internal structure.

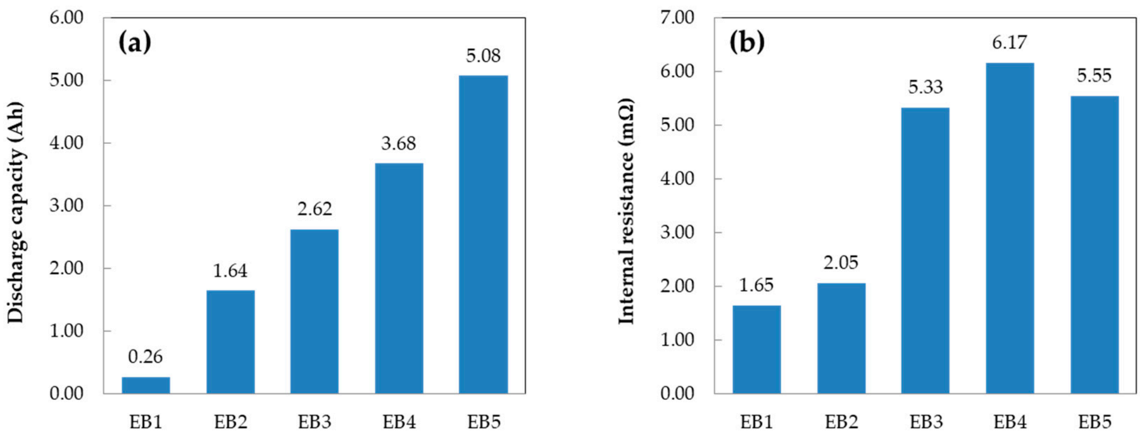

Figure 2. The cell capacity and resistance according to the volume ratio of battery capacitor and supercapacitor in a composite cell. (**a**) capacity; (**b**) resistance.

Figure 3 illustrates the discharge curves of the individual battery capacitor and supercapacitor cells, as well as the composite cells. Supercapacitors exhibit a linear–discharge curve that depends on the voltage since ions in the electrolyte are adsorbed/desorbed on the surfaces of the anode and cathode electrodes, resulting in low voltage drop due to low resistance. Conversely, a battery capacitor has a flat section in its discharge curve since Li-ions intercalate/deintercalate from the positive and negative electrode materials at a specific voltage instead of a linear–discharge curve [25]. Figure 3b represents an enlarged section of the red circle depicted in Figure 3a. It specifically focuses on the IR-drop region at the initial stage of discharge. The initial voltage during discharge increases as the volume ratio of the supercapacitor increases in the composite cell. This occurred because the battery capacitor changed to a supercapacitor–discharge curve in the initial discharge voltage range due to low energy.

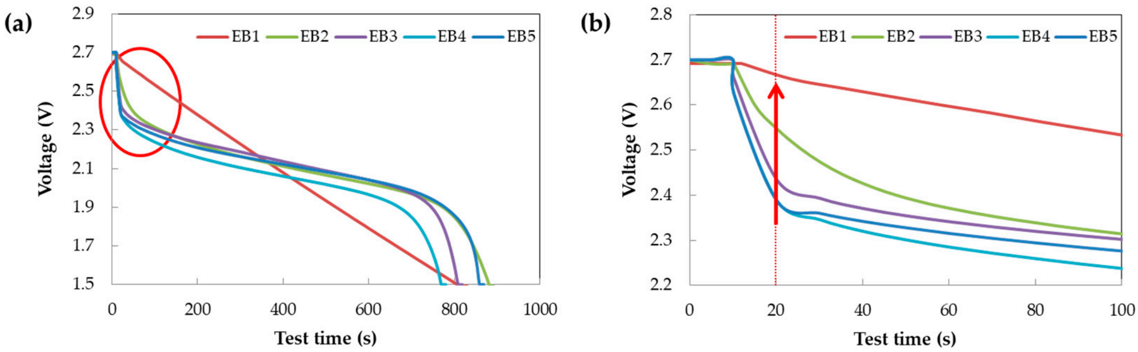

Figure 3. The discharge curve according to the volume ratio of battery capacitor and supercapacitor in a composite cell. (**a**) discharge curve; (**b**) the part of the red circle in figure (**a**).

Figure 4 illustrates the rate of the capacity and resistance change in individual battery capacitor cells, supercapacitor cells, and composite cells in relation to the applied current. In Figure 4a, the rate of capacitance change tended to decrease as the current increased, while in Figure 4b, the resistance change rate decreased, except for supercapacitor cells. The findings revealed that the capacity change rate increased as the volume ratio of the supercapacitor within the composite cell, combining both the battery capacitor and supercapacitor, increased. This suggests that the high-power characteristics of supercapacitors contribute to enhancing the performance of battery capacitors, particularly at high currents.

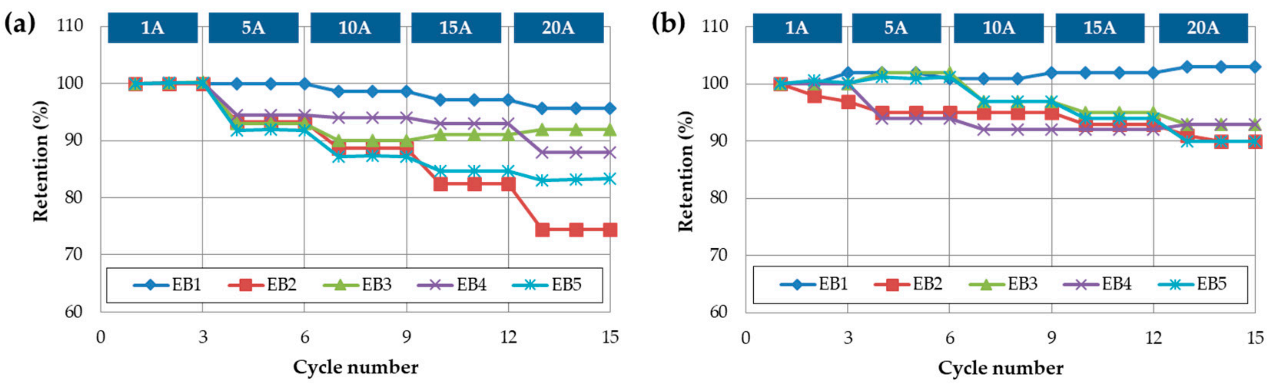

Figure 4. The c-rate properties according to the volume ratio of battery capacitor and supercapacitor in a composite cell ((**a**) Capacity; (**b**) Internal resistance).

The individual battery capacitor and supercapacitor cells, as well as the composite cells, are manufactured with identical sizes but are also assembled with varying internal volume ratios. In Figure 5a, when evaluating the c-rate of the cell using a charge/discharge current ranging from 1 A to 20 A, the current per unit volume remains constant. However,

Figure 5b illustrates a comparison of the applied current and the cell capacity. It can be observed that the cell composed solely of the supercapacitor received 76.09C at 20 A, whereas the battery capacitor received only 3.94C. Despite the identical current per unit volume, the current received in terms of capacity differed significantly due to variations in the capacity resulting from the volume ratio of the composite cell.

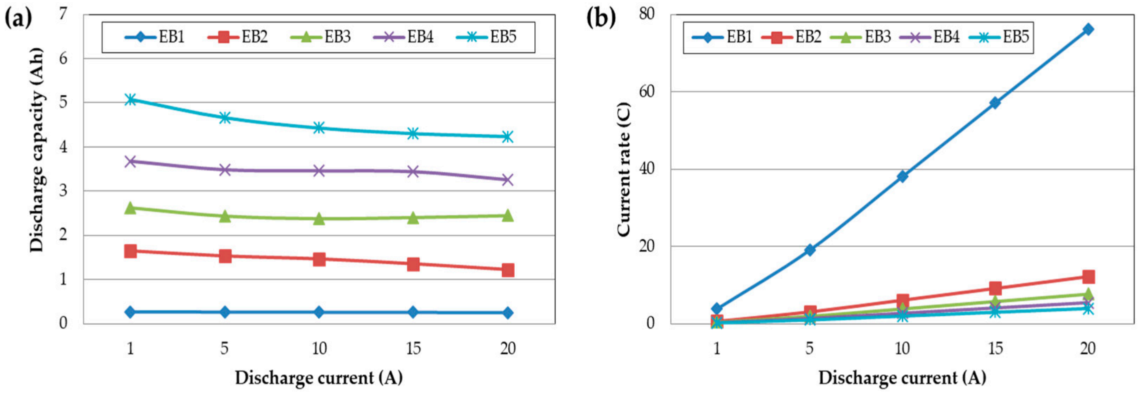

Figure 5. The cell capacity and current rate according to current density. (**a**) capacity; (**b**) current rate.

To evaluate the lifespan characteristics of individual battery capacitor cells, supercapacitor cells, and composite cells, a life evaluation was conducted at room temperature using a current of 20C, as depicted in Figure 6. When a cell consisted solely of a battery capacitor, the capacity retention rate dropped below 80% compared to the initial capacity after approximately 4200 cycles of charging and discharging. However, it can be confirmed that the number of cycles in which the capacity retention rate fell below 80% increased when the supercapacitor was added according to the volume ratio of the composite cell. Figure 5b illustrates that the C-rate received by the cell increased as the volume ratio occupied by the supercapacitor within the cell increased. Typically, the lifespan of energy storage devices deteriorated as the C-rate increased. However, when battery capacitors were combined with supercapacitors, the lifespan actually improved. This could be attributed to the excellent high-output characteristics of the supercapacitor, which reduced heat generation within the composite cell during the charging and discharging process. As a result, the lifespan of the composite cell was extended.

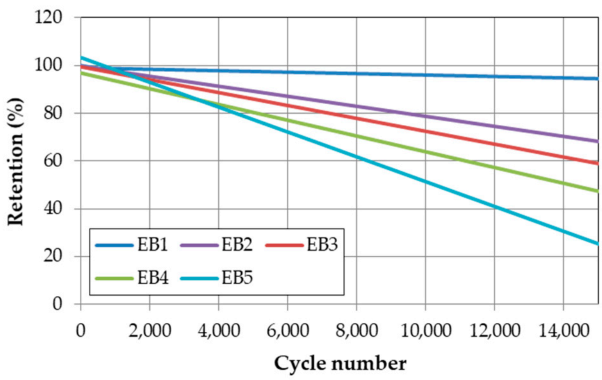

Figure 6. The cycle properties according to the volume ratio of the battery capacitor and supercapacitor in a composite cell.

Additionally, Figure 7 shows the temperature of the cell measured using a thermal imaging camera during the cycle evaluation. Typically, a thermal imaging camera evaluates the temperature at 5 to 8 points and displays it on the screen. Figure 8 displays the highest and lowest temperature points of the cell during life evaluation. The surface temperature of the EB5 cell, which utilizes only battery capacitors, was measured between 43 and

48 °C during the life evaluation. As the ratio of the supercapacitor in the cell increased, the cell's temperature decreased. Since cell temperature is a significant factor affecting lifespan characteristics, combining a supercapacitor reduces the temperature during the charging and discharging process, thereby improving the lifespan characteristics.

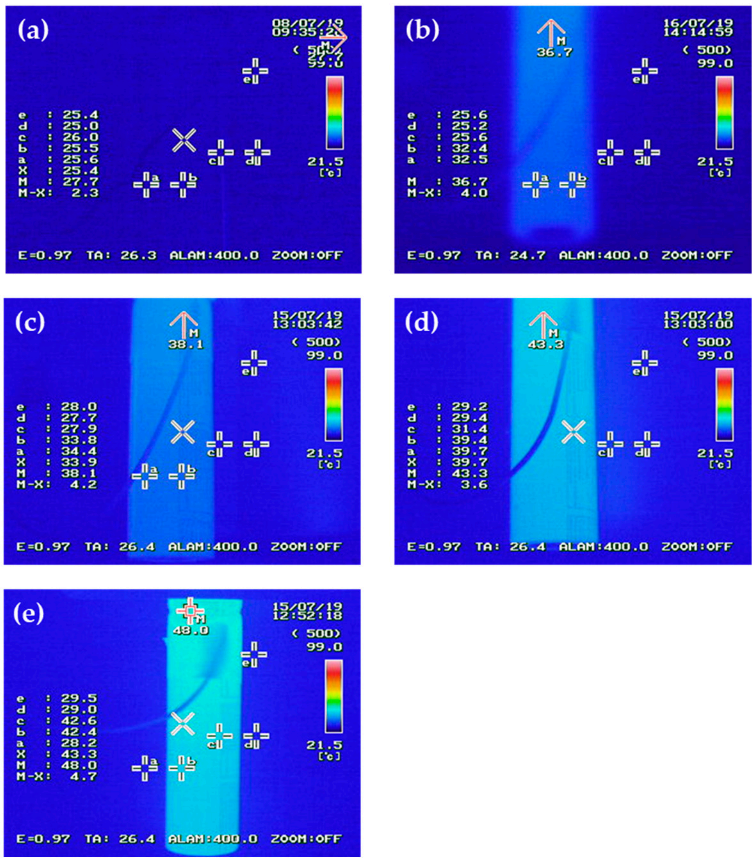

Figure 7. The cell temperature according to cycle measurement: (**a**) EB1, (**b**) EB2, (**c**) EB3, (**d**) EB4, (**e**) EB5.

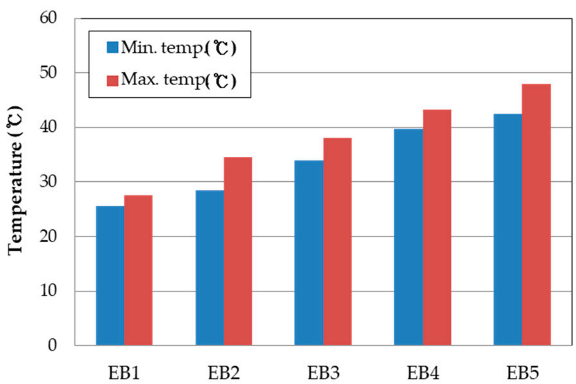

Figure 8. The maximum and minimum temperature of the composite cell measured during cycle measurement.

To investigate the current behavior during the charging and discharging of battery capacitors and supercapacitors connected in parallel, individual currents were measured using an oscilloscope, and the results are depicted in Figure 9. As shown in Figure 9d, during the initial charging, the current flowed into the supercapacitor, which gradually decreased over time. On the contrary, in the case of a battery capacitor, the initial charging current was small but increased over time, resulting in a reversal of the charging current magnitude. According to the current distribution law, the majority of the charging current initially flows into the supercapacitor due to its low resistance. However, as the supercapacitor becomes charged, the charging current shifts toward the battery capacitor. The specifics of the initial current received by the supercapacitor and battery capacitor in Figure 9a–c, along with information on the time when the current was reversed, are presented in Table 2. The larger the volume ratio of the supercapacitor in the composite cell, the longer it took for the charging current to reverse. Additionally, with a larger volume ratio of the supercapacitor, the current received by the battery capacitor decreased at an earlier stage, leading to an improvement in the lifespan of the composite cell [26].

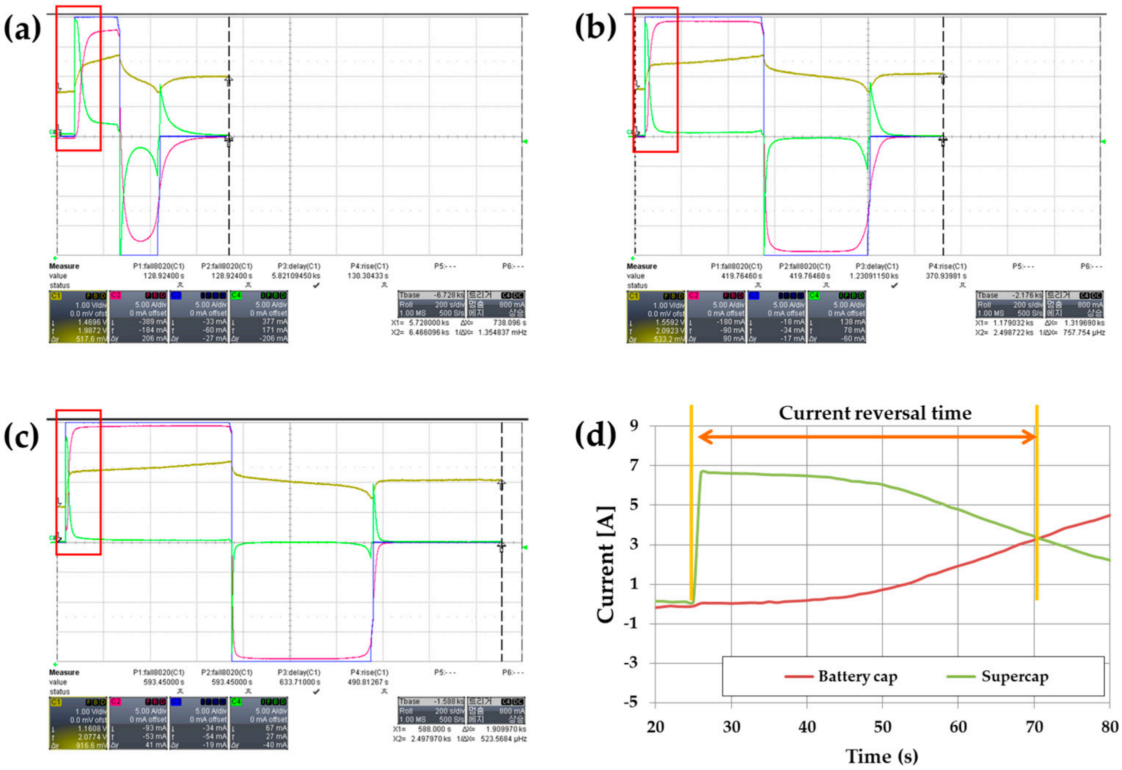

Figure 9. The current distributed between the battery capacitor and supercapacitor when charging and discharging the composite cell: (**a**) EB2, (**b**) EB3, (**c**) EB4, (**d**) Enlarged part of current behavior.

Table 2. Distributed current properties of battery capacitors and supercapacitors when charging and discharging complex cells.

Item	EB2		EB3		EB4	
	Super Capacitor	Battery Capacitor	Super Capacitor	Battery Capacitor	Super Capacitor	Battery Capacitor
Percentage of supercap in total capacity (%)	14.7	85.3	5.4	94.6	1.9	98.1
Initial current (A)	19.56	0.44	18.86	1.14	17.65	2.32
Initial current rate (%)	97.8	2.2	94.3	5.7	88.2	11.8
Time for the current to reverse (s)	28.43		17.12		12.18	

Figure 10 presents the electrical characteristics of the composite cell as a function of the volume ratio of the supercapacitor and battery capacitor based on our measurements. As the volume occupied by the supercapacitor increased in the composite cell, the capacity, resistance, and energy density per unit volume tended to decrease, while the lifespan, output characteristics, and cost of the energy storage tended to increase. Due to the different characteristics of the supercapacitor and battery capacitor, the composite cell exhibited various electrical characteristics depending on the volume ratio. Consequently, it was possible to design a new type of energy storage device with complementary characteristics by adjusting the volume ratio of the components.

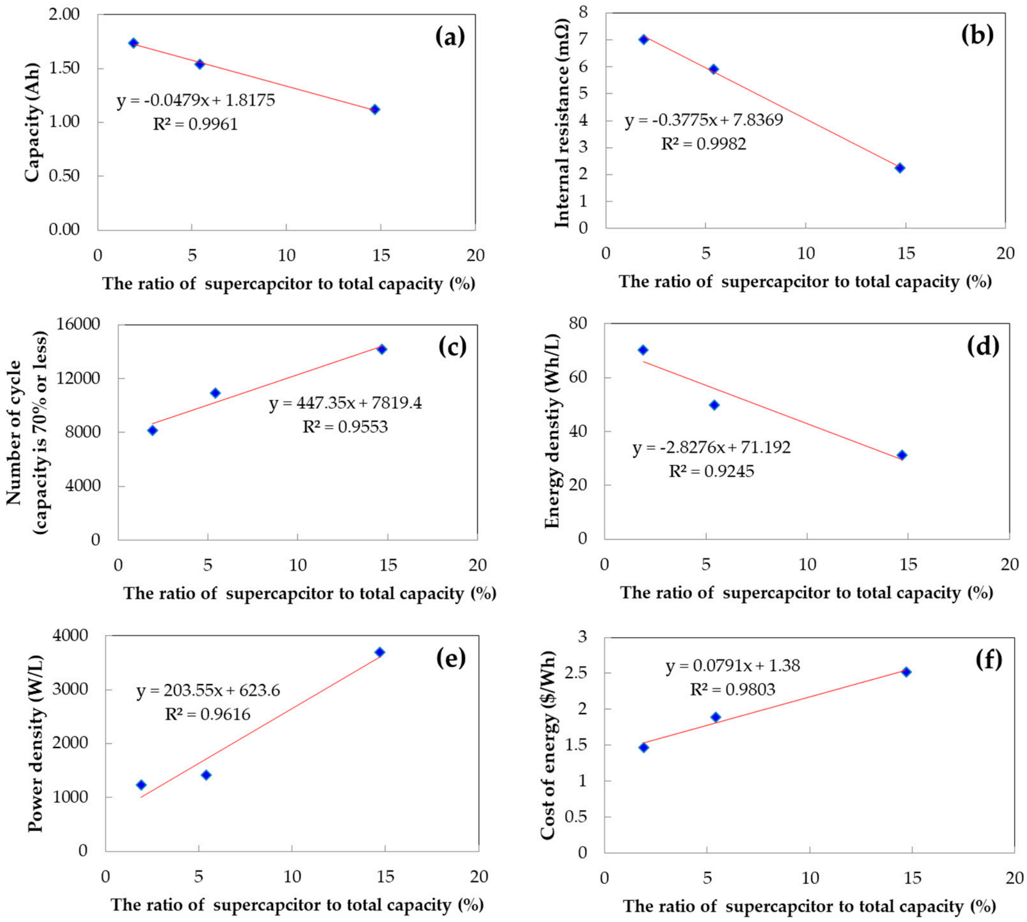

Figure 10. The trend of characteristics according to the volume ratio of battery capacitor and supercapacitor in composite cell. (**a**) capacity; (**b**) resistance; (**c**) number of cycle; (**d**) energy density; (**e**) power density; (**f**) cost of energy.

4. Conclusions

The conclusion of this dissertation proposes the development of a new type of energy storage device through the internal parallel connection of two different types of energy storage devices. The study shows that supercapacitors and battery capacitors can complement each other's characteristics when compounded, with the battery capacitor affecting energy improvement and the supercapacitor affecting resistance and lifespan characteristic improvements. The volume ratio of the two storage devices affects the characteristics of the complex cell, and this study allowed for the quantification of the capacity, resistance, lifespan, energy density, power density, and cost of a composite cell based on the volume ratio. From the perspective of users employing conventional energy devices, cells are designed based on considerations such as capacity, lifespan, energy output, price, and other factors, with each application requiring distinct key characteristics. Through our research efforts, we have obtained essential data for designing cells tailored to specific applications. Consequently, we have successfully developed a novel energy storage device that integrates both supercapacitors and battery capacitors, thereby optimizing performance and functionality for various applications. This breakthrough marks a significant advancement in the field of energy storage technology.

Author Contributions: Conceptualization, J.-K.L. and J.-R.Y.; methodology, J.-K.L. and J.-R.Y.; software, J.-K.L.; validation, J.-K.L. and J.-R.Y.; formal analysis, J.-K.L. and J.-R.Y.; investigation, J.-K.L. and J.-R.Y.; resources, J.-K.L. and J.-R.Y.; data curation, J.-K.L. and J.-R.Y.; writing—original draft preparation, J.-K.L.; writing—review and editing, J.-K.L. and J.-R.Y.; visualization, J.-K.L.; supervision, J.-K.L. and J.-R.Y.; project administration, J.-K.L. and J.-R.Y.; funding acquisition, J.-K.L. and J.-R.Y. All authors have read and agreed to the published version of the manuscript.

Funding: This work was supported by the Technology Innovation Program (10062226, The development of battery capacitor (58 Wh/L) composed of a graphene and lithium transition metal oxide-based flexible electrode for IoT device) funded by the Ministry of Trade, Industry & Energy (MOTIE, Korea).

Data Availability Statement: Data are available on request.

Conflicts of Interest: The authors declare no conflict of interest.

References

1. Cheng, F.; Chen, J.; Liang, J. Functional materials for rechargeable batteries vs. supercapacitors. *Prog. Mater. Sci.* **2011**, *56*, 917–1013.
2. Chmiola, J.; Yushin, G.; Gogotsi, Y.; Portet, C.; Simon, P.; Taberna, P.L. Anomalous increase in carbon capacitance at pore sizes less than 1 nanometer. *Science* **2006**, *313*, 1760–1763. [CrossRef]
3. Huang, Y.; Zhu, M.; Zhu, K.; Yang, Q.H.; Wang, J. Mechanisms of pseudocapacitive energy storage in transition metal oxides/hydroxides. *Adv. Energy Mater.* **2015**, *5*, 1500930.
4. Miller, J.R.; Simon, P. Electrochemical capacitors for energy management. *Science* **2008**, *321*, 651–652. [CrossRef]
5. Xu, J.; Wang, X.; Shen, P.K. Recent progress on 2D materials for supercapacitor electrodes: From rational synthesis to electrochemical performance. *Adv. Energy Mater.* **2017**, *7*, 1700626.
6. Larcher, D.; Tarascon, J.M. Towards greener and more sustainable batteries for electrical energy storage. *Nat. Chem.* **2015**, *7*, 19–29. [CrossRef]
7. Gogotsi, Y.; Simon, P. True performance metrics in electrochemical energy storage. *Science* **2011**, *334*, 917–918. [CrossRef]
8. Augustyn, V.; Simon, P.; Dunn, B. Pseudocapacitive oxide materials for high-rate electrochemical energy storage. *Energy Environ. Sci.* **2014**, *7*, 1597–1614. [CrossRef]
9. Pandolfo, A.G.; Hollenkamp, A.F. Carbon properties and their role in supercapacitors. *J. Power Sources* **2006**, *157*, 11–27. [CrossRef]
10. Simon, P.; Gogotsi, Y. Materials for electrochemical capacitors. *Nat. Mater.* **2013**, *7*, 845–854. [CrossRef]
11. Wang, Y.; Zhang, T.; Xiao, J.; Tian, X.; Yuan, S. Enhancing electrochemical performance of ultrasmall Fe_2O_3-embedded carbon nanotubes via combusting-induced high–valence dopants. *J. Mater. Sci. Technol.* **2023**, *134*, 142–150. [CrossRef]
12. Wang, Y.; Xiao, J.; Wang, H.; Zhang, T.C.; Yuan, S. Binary doping of nitrogen and phosphoorus into porous carbon: A novel di-functional material for enhancing CO_2 capture and supercapacitance. *J. Mater. Sci. Technol.* **2022**, *99*, 73–81. [CrossRef]
13. Khalid, M. A Review on the Selected Applicaiotns of Battery-Supercapacitor Hybrid Energy Storage Systems for Microgrids. *Energies* **2019**, *12*, 4559. [CrossRef]
14. Kouchachvili, L.; Yaici, W.; Entchev, E. Hybrid battery/supercapacitor energy storage system for the electric vehicles. *J. Power Sources* **2018**, *374*, 237–248. [CrossRef]
15. Chen, Q.; Li, Y.; Wang, Q.; Li, X. A comparative study of $Li_4Ti_5O_{12}$ and graphite anodes for high-performance lithium-ion batteries. *J. Power Sources* **2015**, *274*, 823–829.
16. Zhang, X.; Lu, L.; Liu, G. Comparative study of graphite and $Li_4Ti_5O_{12}$ anodes for lithium-ion batteries. *J. Power Sources* **2009**, *189*, 867–870.
17. Li, Z.; Li, J.; Liang, J.; Li, Y.; Li, X.; Li, Z.; Wang, Q. A review of the research progress on composite energy storage systems based on supercapacitors and batteries. *Renew. Sustain. Energy Rev.* **2019**, *103*, 267–291.
18. Liang, Y.; Xu, Z.; Yang, L.; Zhang, L. A review of composite energy storage system based on supercapacitors and batteries. *J. Power Sources* **2020**, *472*, 228499.
19. Yang, C.; Chen, X.; Huang, Y.; Chen, Z. A review of hybrid energy storage systems based on supercapacitors and batteries. *Sustain. Energy Technol. Assess.* **2017**, *20*, 14–29.
20. Gu, H.; Wang, H.; Chen, Z.; Lin, L.; Guo, X. Enhanced electrochemical performance of supercapacitor by hybridizing with lithium-ion battery. *Electrochim. Acta* **2018**, *283*, 1478–1484.
21. Xiong, J.; Wang, H.; Liu, Y.; Lin, H.; Wang, X. Synergetic effects of hybridizing supercapacitors and batteries in energy storage. *Appl. Energy* **2018**, *211*, 702–716.
22. Saeed, S.; Liu, Z.; Li, X.; Jiao, K. Recent advances in hybrid energy storage systems based on supercapacitors and batteries: A review. *Renew. Sustain. Energy Rev.* **2021**, *135*, 110153.
23. Wang, H.; Gu, H.; Chen, Z.; Guo, X. Review on the research progress of hybrid supercapacitor–battery energy storage system. *Energy Technol.* **2019**, *7*, 1900399.

24. Wang, Y.; Zhou, Q.; Ma, X.; Zhang, J.; Li, W.; Li, G. A review on hybrid energy storage systems combining battery and supercapacitor. *Energy Convers. Manag.* **2019**, *197*, 111961. [CrossRef]
25. Lota, G.; Zhao, X.; Zou, L. Recent advances in hybrid supercapacitors: A brief review. *Nano Energy* **2015**, *13*, 574–583.
26. Huang, J.; Wu, J.; Zeng, X.; Zhang, B.; Hu, J. Recent advances in hybrid supercapacitor-battery systems for energy storage. *J. Energy Storage* **2019**, *25*, 100831.
27. Zhang, J.; Shang, Y.; Hu, M.; Zhang, Y.; Wang, H.; Ma, J. Analysis of the charging and discharging characteristics of a lithium-ion battery-supercapacitor hybrid energy storage system. *J. Power Sources* **2018**, *387*, 66–73.
28. Wang, W.; Luo, J.; Li, J.; Chen, J. Investigation of the current distribution in a hybrid energy storage system combining supercapacitors and batteries. *J. Power Sources* **2014**, *247*, 489–495.